Arrestin Recruitment to C-C Chemokine Receptor 5: Potent C-C Chemokine Ligand 5 Analogs Reveal Differences in Dependence on Receptor Phosphorylation and Isoform-Specific Recruitment Bias [S]

Elsa Martins, Hellena Brodier, Irène Rossitto-Borlat, Ilke Ilgaz, Mélanie Villard, and Oliver Hartley

Department of Pathology and Immunology, Faculty of Medicine, University of Geneva, Geneva, Switzerland

ABSTRACT

C-C chemokine receptor 5 (CCR5) is a chemokine receptor belonging to the G protein–coupled receptor (GPCR) superfamily. An established anti–human immunodeficiency virus drug target, CCR5 is attracting significant additional interest in both cancer and neuroinflammation. Several N-terminally engineered analogs of C-C chemokine ligand 5 (CCL5), a natural ligand of CCR5, are highly potent CCR5 inhibitors. The inhibitory mechanisms of certain analogs relate to modulation of receptor desensitization, but the cellular and molecular mechanisms have not been fully elucidated. Here we made use of a collection of CCR5 phosphorylation mutants and arrestin variants to investigate how CCL5 analogs differ from CCL5 in their capacity to elicit both CCR5 phosphorylation and arrestin recruitment, with reference to the current "core" and "tail" interaction model for arrestin-GPCR interaction. We showed that CCL5 recruits both arrestin 2 and arrestin 3 to CCR5 with recruitment, particularly of arrestin 2, strongly dependent on the arrestin tail interaction. 5P12–RANTES does not elicit receptor phosphorylation or arrestin recruitment. In contrast, PSC-RANTES induces CCR5 hyperphosphorylation, driving enhanced arrestin recruitment with lower dependence on the arrestin tail interaction. 5P14-RANTES induces comparable levels of receptor phosphorylation to CCL5, but arrestin recruitment is absolutely dependent on the arrestin tail interaction, and in one of the cellular backgrounds used, recruitment showed isoform bias toward arrestin 3 versus arrestin 2. No evidence for ligand-specific differences in receptor phosphorylation patterns across the four implicated serine residues was observed. Our results improve understanding of the molecular pharmacology of CCR5 and help further elucidate the inhibitory mechanisms of a group of potent inhibitors.

SIGNIFICANCE STATEMENT

C-C chemokine receptor 5 (CCR5) is a key drug target for human immunodeficiency virus, cancer, and inflammation. Highly potent chemokine analog inhibitors act via the modulation of receptor desensitization, a process initiated by the recruitment of arrestin proteins. This study shows that potent C-C chemokine ligand 5 analogs differ from each other and from the parent chemokine in the extent and quality of CCR5-arrestin association that they elicit, providing valuable insights into CCR5 pharmacology and cell biology that will facilitate the development of new medicines targeting this important receptor.

Introduction

C-C chemokine receptor 5 (CCR5) is a chemokine receptor that belongs to the G protein–coupled receptor (GPCR) superfamily. Although its main physiologic role is in the recruitment of effector cells in inflammatory responses (Wong and Fish, 2003), CCR5 is also the principal coreceptor used by human immunodeficiency virus (HIV) to infect target cells, and in addition to being a validated drug target for both prevention and treatment of HIV (Carrington et al., 1999; Gallo et al., 2003), it is emerging as a promising target in both oncology (Aldinucci and Casagrande, 2018) and neuroinflammation (Martin-Blondel et al., 2016). C-C chemokine ligand 5 (CCL5) is one of the natural ligands of CCR5, and a number of N-terminally modified CCL5 analogs with highly potent anti-HIV activity have been described (Hartley et al., 2004; Gaertner et al., 2008).

Although these analogs only differ from each other at a few positions in the N-terminal region of the chemokine, their inhibitory mechanisms are strikingly different (Table 1). Whereas 5P12–regulated on activation normal T cell expressed and secreted (RANTES) acts via high-affinity steric blockade of CCR5 at the cell surface (Gaertner et al., 2008; Colin et al., 2013;

[S] This article has supplemental material available at molpharm.aspetjournals.org.

ABBREVIATIONS: Arr2, arrestin 2; Arr3, arrestin 3; AU, arbitrary units; AUC, area under the curve; BRET, bioluminescence resonance energy transfer; BSA, bovine serum albumin; CCL5, C-C chemokine ligand 5; CCR5, C-C chemokine receptor 5; CI, confidence interval; GPCR, G protein–coupled receptor; HEK, human embryonic kidney; HIV, human immunodeficiency virus; HRP, horseradish peroxidase; KO, knockout; P/S, penicillin-streptomycin; PD-CCR5, "phospho-dead" variant of CCR5; PSC-RANTES, n-nonanoyl-thioprolyl-cyclohexylglycyl–RANTES; RANTES, regulated on activation normal T cell expressed and secreted; WT, wild type; YFP, yellow fluorescent protein.

TABLE 1
Structure of recombinant chemokine analogs

Compound	Structure	Inhibitory mechanism	References
CCL5	SPYSSDTTP-CCL5 (10–68)	Cell surface steric blockade plus intracellular sequestration (trans-Golgi network)	Trkola et al., 1998; Escola et al., 2010
PSC-RANTES	PSC-SSDTTP-CCL5 (10–68)	Enhanced intracellular sequestration (trans-Golgi network)	Hartley et al., 2004; Escola et al., 2010
5P14-RANTES	QGPPLMSLQV-CCL5 (10–68)	Intracellular sequestration (endosome recycling complex)	Gaertner et al., 2008; Bönsch et al., 2015
5P12-RANTES	QGPPLMATQS-CCL5 (10–68)	Cell surface steric blockade	Gaertner et al., 2008

Zheng et al., 2017), the inhibitory mechanisms of n-nonanoyl-thioprolyl-cyclohexylglycyl–RANTES (PSC-RANTES) (Hartley et al., 2004) and 5P14-RANTES (Gaertner et al., 2008) involve modulation of the CCR5 desensitization process, leading to removal of CCR5 from the cell surface (Hartley et al., 2004; Gaertner et al., 2008; Escola et al., 2010; Colin et al., 2013; Jin et al., 2014). PSC-RANTES elicits enhanced CCR5 internalization compared with CCL5 (Gaertner et al., 2008), and 5P14-RANTES elicits sorting of internalized receptors to an intracellular site (endosome recycling complex) different from that at which receptors internalized by CCL5 and PSC-RANTES accumulate (trans-Golgi network) (Bönsch et al., 2015).

Central to the GPCR desensitization process is the recruitment of arrestin proteins, which initiate receptor endocytosis and orchestrate postendocytic trafficking (DeWire et al., 2007; Lefkowitz, 2007; Eichel and von Zastrow, 2018; Rajagopal and Shenoy, 2018). Most nonvisual GPCRs make use of two arrestin isoforms, arrestin 2 and arrestin 3 (also known as β-arrestin-1 and β-arrestin-2) (Alvarez, 2008; Peterson and Luttrell, 2017). Agonist-induced phosphorylation of GPCRs at sites in the intracellular C-terminal region of the receptor, catalyzed by G protein–coupled receptor kinases, is generally recognized as an important first step in arrestin recruitment (Gurevich and Gurevich, 2006), although individual GPCRs show differences in the extent to which phosphorylation is required for this process (Richardson et al., 2003; Chen et al., 2004; Jala et al., 2005; Gimenez et al., 2012). Agonist-driven CCR5 phosphorylation has been shown to be directed to four serine residues located in the C-terminal tail domain of the receptor, Ser[336], Ser[337], Ser[342], and Ser[349] (Oppermann et al., 1999). Studies of restricted sets of CCR5 Ser-Ala mutants at these sites have indicated that phosphorylation is required for both robust recruitment of arrestins (Kraft et al., 2001; Hüttenrauch et al., 2002) and receptor endocytosis (Kraft et al., 2001).

According to the current model (Eichel et al., 2018; Kahsai et al., 2018; Latorraca et al., 2018), arrestins use two mechanisms for recruitment to activated GPCRs. The "tail interaction" involves destabilization of an internal ionic lock in the arrestin protein by the phosphorylated C-terminal tail region of the receptor, resulting in a conformational change that stabilizes binding to this region of the receptor (Eichel et al., 2018; Kahsai et al., 2018; Latorraca et al., 2018). The "core interaction" involves docking of a conformationally flexible structure on the arrestin protein with structural motifs revealed upon receptor activation that are conserved across the GPCR superfamily (Eichel et al., 2018; Kahsai et al., 2018; Latorraca et al., 2018). Previously published work has

indicated that both the enhanced receptor internalization elicited by PSC-RANTES (Gaertner et al., 2008; Escola et al., 2010) and the modified postendocytic trafficking itinerary driven by 5P14-RANTES (Bönsch et al., 2015) might be explained by differences in the extent and duration of arrestin recruitment, but the molecular mechanisms underlying these differences have yet to be elucidated.

In this study we performed a complete survey of the extent and duration of arrestin recruitment to CCR5 driven by both native CCL5 and CCL5 analogs, focusing on possible differences in levels of recruitment of the two arrestin isoforms, agonist induced receptor phosphorylation, and in the relative importance of tail versus the core interaction.

Materials and Methods

Plasmids

CCR5-RLuc8 Constructs. CCR5 fused via its C terminus to the *Renilla* luciferase variant RLuc8 (Loening et al., 2006) was assembled by polymerase chain reaction and cloned into the pCDNA3.1 expression vector using the XbaI and NotI sites to generate pCDNA3.1-CCR5-RLuc8. CCR5 Ser-to-Ala variants fused via their C termini to RLuc8, including FUGW-PD-CCR5-RLuc8, were cloned into the FUGW lentiviral vector (Lois et al., 2002) using a combination of Gibson assembly (Gibson Assembly Master Mix; New England BioLabs, Ipswich, MA) and site-directed mutagenesis (Quikchange; Agilent, Santa Clara, CA).

Yellow Fluorescent Protein–Arrestin Constructs. An open reading frame encoding yellow fluorescent protein (YFP) fused via its C terminus to arrestin 2 was cloned into the FUGW lentiviral vector (Lois et al., 2002) by Gibson assembly to generate FUGW-YFP–arrestin 2 (Arr2). Site-directed mutagenesis of FUGW-YFP-Arr2 was used to generate FUGW-YFP-R169E-Arr2.

An open reading frame encoding YFP fused via its C terminus to arrestin 3 was assembled by polymerase chain reaction and cloned into the pTRE2hyg vector (Clontech, Mountain View, CA) using the EcoRV site to generate pTRE2-YFP–arrestin 3 (Arr3). YFP-Arr3 was also cloned into the FUGW lentiviral vector (Lois et al., 2002) by Gibson assembly (Gibson Assembly Master Mix; New England BioLabs) to generate FUGW-YFP-Arr3. Site-directed mutagenesis of FUGW-YFP-Arr3 (Quikchange; Agilent) was used to generate FUGW-YFP-Arr3-L69R and FUGW-YFP-D70P-Arr3.

Cell Lines

All cell lines were cultured at 37°C with 5% CO_2, and all cell culture reagents were obtained from Invitrogen (Thermo Fisher Scientific, Waltham, MA).

CHO-CCR5. The CHO-CCR5 clonal cell line used in this study has been described previously (Hartley et al., 2004; Gaertner et al., 2008).

CHO-CCR5-RLuc8 Bioluminescence Resonance Energy Transfer Reporter Cell Lines. Cell lines were generated by transfecting

(X-tremeGENE; Roche, Basel, Switzerland) CHO parental cells with pCDNA3.1-CCR5-RLuc8 plasmid, followed by isolation of a stably transfected clone. The CHO-CCR5-RLuc8 cell line was then either transduced with lentiviral vectors (Naldini et al., 1996) FUGW-YFP-Arr2 or transfected (X-tremeGENE; Roche) with pTRE2-YFP-Arr3 to generate stable clonal bioluminescence resonance energy transfer (BRET) cell lines expressing CCR5-RLuc8 together with either YFP-Arr2 (CHO-CCR5-RLuc8 YFP-Arr2 cells) or YFP-Arr3 (CHO-CCR5-RLuc8 YFP-Arr3 cells). CHO-CCR5-RLuc8 YFP-Arr2 cells were maintained in RPMI supplemented with 10% FBS and 1% geneticin. CHO-CCR5-RLuc8 YFP-Arr3 cells were maintained in RPMI supplemented with 10% FBS, 1% penicillin-streptomycin (P/S), 1% geneticin, and 0.5% hygromycin. The levels of the fusion proteins overexpressed in this background were quantified by Western blot and flow cytometry (see Supplemental Figs. 1 and 2; Supplemental Table 1).

CHO-PD-CCR5-RLuc8 BRET Reporter Cell Lines. The CHO-PD-CCR5-RLuc8 YFP-Arr2 cell line was generated by lentiviral transduction of CHO parental cells with FUGW-PD-CCR5-RLuc8 and FUGW-YFP-Arr2 followed by clonal isolation. Cells were maintained in RPMI supplemented with 10% FBS and 1% P/S. The CHO-PD-CCR5-RLuc8 YFP-Arr3 cell line was generated by lentiviral transduction of CHO-YFP-Arr3 with FUGW-PD-CCR5-Rluc8 followed by clonal isolation. Cells were maintained in RPMI supplemented with 10% FBS, 1% P/S, and 0.5% hygromycin. The levels of the fusion proteins overexpressed in this background were quantified by Western blot and flow cytometry (see Supplemental Figs. 1 and 2; Supplemental Table 1).

Human Embryonic Kidney and Human Embryonic Kidney–Arr2/3–Knockout Cell Lines. The human embryonic kidney (HEK)–Arr2/3–knockout (KO) parental cell line (Alvarez-Curto et al., 2016) was kindly provided by Andrew Tobin (University of Glasgow). Both HEK cells HEK-Arr2/3-KO cells were maintained in RPMI supplemented with 10% FBS and 1% P/S.

Chemokines

Chemokines and chemokine analogs used in this study were prepared by total chemical synthesis as described previously (Hartley et al., 2004; Gaertner et al., 2008).

BRET Assay for Arrestin Recruitment

For dose-response BRET assays using stable CHO-derived cell lines, cells were seeded overnight on white, flat-bottom 96-well plates (50,000 cells per well). Cells were then washed and incubated for 15 minutes with BRET buffer [0.14 M NaCl, 6 mM KCl, 2 mM MgSO$_4$, 15 mM HEPES, 1 g/l glucose, 1% bovine serum albumin (BSA)] containing 5 μM Coelenterazine h. BRET measurements were made prior to and after stimulation with chemokines diluted in BRET buffer or BRET buffer alone using a POLARstar Omega instrument (BMG LABTECH, Ortenberg, Germany).

For single-concentration BRET assays using transiently transfected HEK cells, 12-well plates were seeded (150,000 cells per well) on day 1. On day 2 cells were transfected with appropriate plasmids using jetPRIME (Polyplus transfection; 1.8 μg of each plasmid was used, with a total of 3.6 μg added per well, and a 1:2 DNA: transfection reagent ratio was used, with 7.2 μl of transfection reagent added per well). On day 3, cells were washed with PBS, detached, and resuspended in 1 ml culture medium. Pooled suspensions were then seeded overnight on white, flat-bottom 96-well plates (100 μl per well). On day 4, medium was removed, and cells were incubated for 15 minutes in BRET buffer containing 5 μM Coelenterazine h, with BRET measurements made prior to and after stimulation with either chemokines diluted in BRET buffer or BRET buffer alone.

For dose-response BRET assays using transiently transfected HEK-Arr2/3-KO cells, cells were seeded at a density of 2 million cells in 10 cm Petri dishes on day 1. On day 2, cells were transiently transfected with the appropriate BRET plasmids using jetPRIME (Polyplus transfection) (7.5 μg of each plasmid was used, with a total of

15 μg added per 10 cm dish, and a 1:2 DNA: transfection reagent ratio was used, with 30 μl of transfection reagent added per 10 cm dish). On day 3, cells were washed with PBS, detached, and seeded on a 96-well plate (white, flat bottom) at a cell density of 30,000 cells/well (in a volume of 100 μl/well). On day 4, medium was removed, and cells were incubated for 15 minutes in BRET buffer containing 5 μM Coelenterazine h, with BRET measurements made prior to and after stimulation with either chemokines diluted in BRET buffer or BRET buffer alone. The levels of the fusion proteins overexpressed in this background were quantified by Western blot and flow cytometry (see Supplemental Figs. 1 and 2; Supplemental Table 1).

ELISA Assay for Quantification of CCR5 Phosphorylation

CHO-CCR5 cells were seeded overnight on 24-well plates (100,000–200,000 cells per well). Cells were then washed and incubated with 100 nM of CCR5 ligands diluted in culture medium supplemented with 1% BSA for 1 hour at 37°C. Medium was removed, and cells were incubated with lysis buffer [25 mM Tris, 150 mM NaCl, 1 mM EDTA, 1% NP-40, 5% glycerol, protease/phosphatase inhibitors (Thermo Fisher Scientific)] on a shaker (10 minutes, room temperature). The supernatant was recovered for the ELISA assay.

The wells of a Maxisorb 96-well plate were coated with an anti-CCR5 antibody (5 μg/ml, 3A9; BD Biosciences, San Jose, CA) overnight at 4°C. After a blocking step with PBS-BSA 3% (1 hour, room temperature), the wells were washed three times with wash buffer (25 mM Tris, 150 nM NaCl, 0.1% BSA, 0.05% Tween-20, pH 7.2) prior to loading with the cellular supernatants (1 hour, room temperature). Wells were washed three times and then incubated (1 hour, room temperature) with phospho-specific anti-CCR5 recombinant monoclonal antibodies (1 μg/ml) (https://oap.unige.ch/journals/abrep). Wells were washed three times and then incubated with secondary antibody [goat anti-rabbit conjugated with horseradish peroxidase (HRP); DAKO (Agilent), 1:5000; 30 minutes, room temperature], prior to washing three times and revelation using 3,3′,5,5′-tetramethylbenzidine substrate (Sigma-Aldrich, St. Louis, MO). Reactions were stopped with H$_2$SO$_4$ 2 N, and absorbance at 450 nm was measured. Total protein concentration for each condition was determined using a bicinchoninic acid assay (Sigma-Aldrich). Results were expressed as normalized absorbance signal (absorbance at 450 nm/total protein concentration, microgram per microliter).

Western Blot for Detection of CCR5 and Arrestin Fusion Proteins

For CHO-derived BRET cell lines, cells were cultivated to semiconfluency (approximately 8–10 million cells) in 10 cm Petri dishes on day 1 followed by protein extraction on day 2. HEK-Arr2/3-KO cells were seeded at a density of 2 million cells in 10 cm Petri dishes on day 1. On day 2, cells were transiently transfected with the appropriate BRET plasmids using jetPRIME (Polyplus transfection) (7.5 μg of each plasmid was used, with a total of 15 μg added per 10 cm dish, and a 1:2 DNA: transfection reagent ratio was used, with 30 μl of transfection reagent added per 10 cm dish). On day 3, protein extraction was performed: the dishes were placed on ice, washed two times in cold PBS (1×), and incubated on ice with 1 ml per plate of lysis buffer [Tris 50 mM, 1% NP40 supplemented with Halt Protease inhibitor 1× (Thermo Fisher Scientific)]. The resulting supernatant was centrifuged for 10 minutes at 14,000 rpm in a bench top centrifuge, and lysates were dosed for protein content using Pierce BCA Protein Assay Kit (Thermo Fisher Scientific). Samples corresponding to 10 μg of protein per lane in NuPAGE LDS Sample Buffer (Invitrogen) and dithiothreitol (final concentration of 0.1 M) were loaded on a 15-lane Nu-PAGE 4%–12% Bis-Tris gel (Invitrogen).

Lysates were heated to 100°C for 1 minute prior to loading. Electrophoresis was performed in MES SDS running buffer (Novex, Thermo Fisher Scientific) for 35 minutes at 200 V. After electrophoresis, samples were transferred using iBlot 2NC Regular stacks

(Invitrogen). Membranes were blocked for 1 hour at room temperature in PBS-BSA-T (PBS, 3% BSA, 0.1% Tween). After one washing step in PBS-BSA-T (10 minutes) and two washing steps in PBS-Tween 0.1% (10 minutes), membranes were incubated for 1 hour at room temperature with primary antibody [rat monoclonal anti-CCR5, HEK/1/85a; Bio-Rad (Hercules, CA), diluted at 1:30,000 in PBS-BSA-T; rabbit polyclonal anti–β-actin, ab8227; Abcam (Cambridge, MA), diluted at 1:2500 in PBS-BSA-T; mouse anti-GFP, 11814460001; Roche, diluted at 1:2000 in PBS-BSA-T] followed by one washing step in PBS-BSA-T (10 minutes) and two washing steps in PBS-T (10 minutes). Membranes were then incubated for 1 hour at room temperature with the secondary antibodies (goat anti-rat HRP, APB6P; Chemicon (Thermo Fisher Scientific); goat anti-rabbit HRP, A0545; Sigma; or goat anti-mouse HRP, A5278; Sigma, all diluted at 1:2500) in PBS-BSA-T. After one washing step in PBS-BSA-T (10 minutes) and two washing steps in PBS-T (10 minutes),

membranes were developed using WesternBright Quantum Western blotting detection kit (1:1).

Flow Cytometry for Detection of CCR5 and Arrestin Fusion Proteins

Cells were resuspended in buffer (PBS $1\times$, 1% BSA, 0.05% NaN_3), and a total of 250,000 cells in a volume of 100 μl was added to each well of a 96-well plate. For CCR5-RLuc8 detection, cells were incubated with an anti-CCR5 monoclonal antibody directly labeled with allophycocyanin (2D7-APC; Bio-Rad) on ice for 45 minutes. For YFP-arrestin detection, direct measurement of YFP was performed. Fluorescence was recorded on the allophycocyanin (excitation: 638 nm/emission: 660 nm) and phycoerythrin (excitation: 488 nm/emission: 585 nm) channels. Twenty thousand events were collected per well.
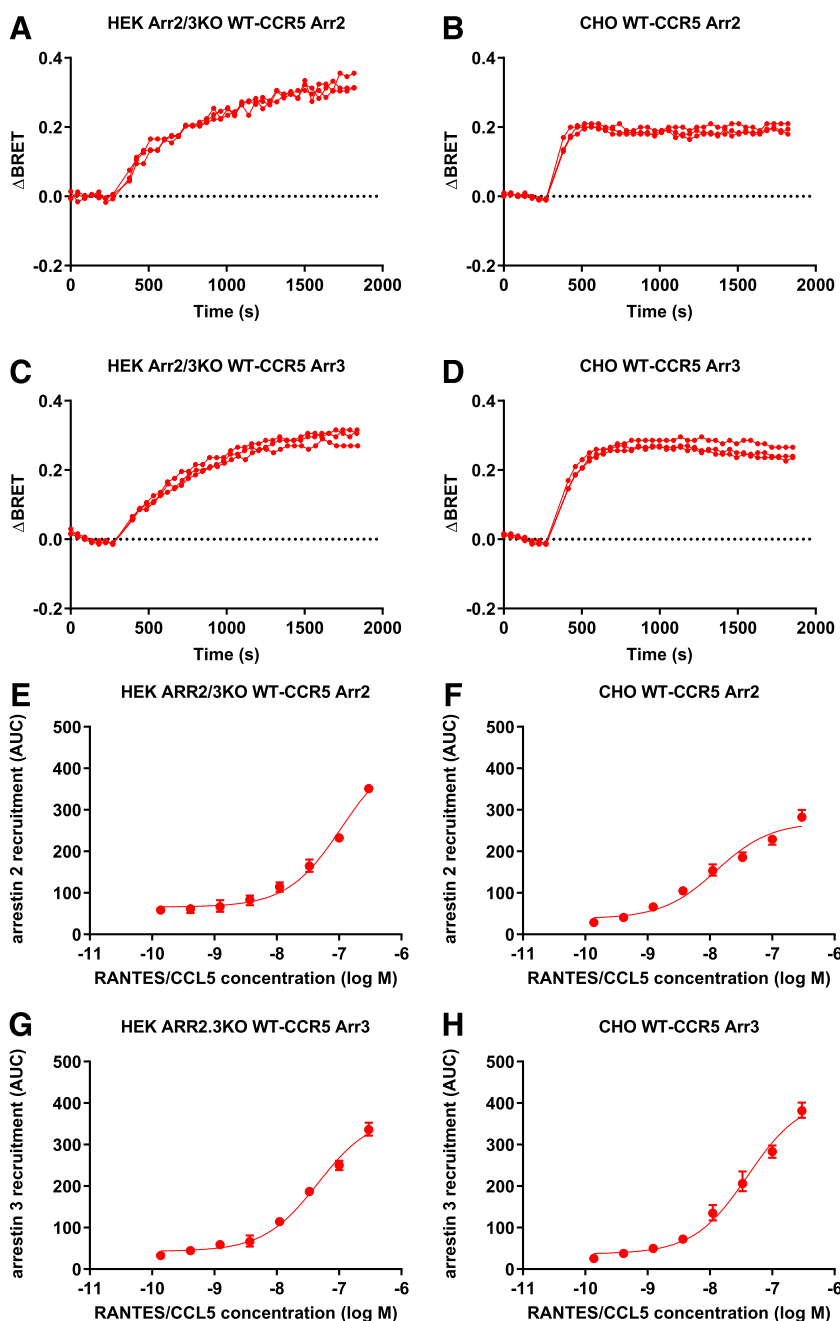

Fig. 1. CCL5-induced recruitment of arrestin 2 and arrestin 3 to WT-CCR5. (A–D) BRET assays were performed by treating cells expressing WT-CCR5-RLuc8 together with YFP-Arr2 or YFP-Arr3 (as indicated) with CCL5 at a concentration of 300 nM for 40 cycles of 45 seconds (chemokine addition after seven cycles). Data are shown as ΔBRET and expressed as AU. Individual traces of the time courses are shown (n = 3). (E–H) BRET assays were performed by treating HEK-Arr2/3-KO or CHO cells expressing WT-CCR5-RLuc8 together with YFP-Arr2 or YFP-Arr3 (as indicated) with CCL5 at the indicated concentrations for 40 cycles of 45 seconds (chemokine addition after seven cycles). Data are shown as AUC (mean ± S.D., n = 3). Fitted curves were obtained by a nonlinear regression analysis [log(agonist) vs. response (three parameters)] using Prism.

Statistical Analysis

All statistical analyses were performed using Prism 8 (GraphPad, La Jolla, CA).

Results

CCL5 Elicits Dose-Dependent Recruitment of Both Arrestin Isoforms. We first performed BRET-based arrestin recruitment assays on wild-type (WT) CCR5 using 1) transiently transfected HEK cells in which both endogenous arrestin isoforms have been knocked out (HEK-Arr2/3-KO) (Alvarez-Curto et al., 2016), eliminating potential interference in BRET signaling by endogenous arrestins, and 2) a stably transduced clonal CHO cell line, providing the same cellular background to that used in several previous studies of CCR5

agonist binding, agonist-mediated endocytosis and postendocytic trafficking (Escola et al., 2010; Bönsch et al., 2015) (Fig. 1).

Recruitment of both arrestin isoforms was observed in response to 300 nM CCL5, with BRET signals approaching a plateau over the 20-minute time course in the HEK-Arr2/3-KO background and more rapidly (within approximately 5 minutes) in the CHO background (Fig. 1, A–D). Dose-response experiments over a range of CCL5 concentrations, using BRET signal area under the curve (AUC) over 20-minute exposure revealed similar responses for the two arrestin isoforms in both cellular backgrounds, with fitted EC_{50} values of 110 nM [95% confidence interval (CI) varying from 77 to 159 nM] and 45 nM (95% CI: 35–60 nM), respectively, for arrestin 2 and arrestin 3 on the HEK-Arr2/3-KO background (Fig. 1, E
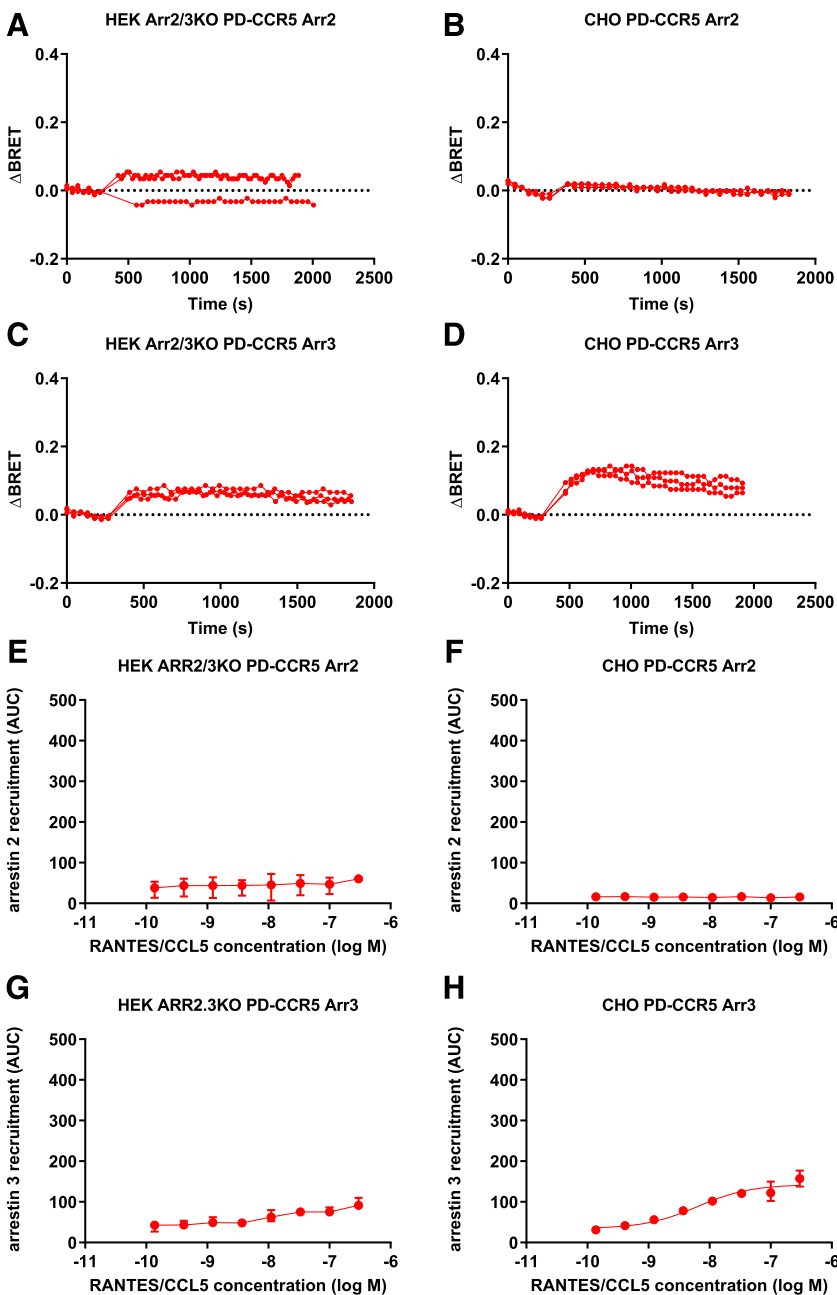

Fig. 2. CCL5-induced recruitment of arrestin 2 and arrestin 3 to PD-CCR5. (A–D) BRET assays were performed by treating cells expressing PD-CCR5-RLuc8 together with YFP-Arr2 or YFP-Arr3 (as indicated) with CCL5 at a concentration of 300 nM for 40 cycles of 45 seconds (chemokine addition after seven cycles). Data are shown as ΔBRET and expressed as AU. Individual traces of the time courses are shown ($n = 3$). (E–H) BRET assays were performed by treating HEK-Arr2/3-KO or CHO cells expressing PD-CCR5-RLuc8 together with YFP-Arr2 or YFP-Arr3 (as indicated) with CCL5 at the indicated concentrations for 40 cycles of 45 seconds (chemokine addition after seven cycles). Data are shown as AUC (mean ± S.D., $n = 3$). Fitted curves (H) were obtained by a nonlinear regression analysis [log(agonist) vs. response (three parameters)] using Prism.

and G), and 13 nM (95% CI: 7.9–21 nM) and 40 nM (95% CI: 29–56 nM), respectively, on the CHO background (Fig. 1, F and H).

CCL5-Elicited Arrestin Recruitment Is Strongly Dependent on CCR5 Phosphorylation. To evaluate the extent to which CCL5-mediated arrestin recruitment is dependent on agonist-elicited receptor phosphorylation, we next performed arrestin recruitment experiments using a "phospho-dead" variant of CCR5 (PD-CCR5) in which each of the four serine residues known to be subject to agonist-induced phosphorylation (Oppermann et al., 1999) was mutated to alanine. Time-course experiments using CCL5 at 300 nM showed that arrestin 2 recruitment is fully attenuated in both the HEK-Arr2/3-KO and the CHO backgrounds (Fig. 2, A and B) and that arrestin 3 recruitment is strongly reduced in both backgrounds (Fig. 2, C and D), with a lower plateau level of arrestin association observed for the HEK-Arr2/3-KO background (Fig. 2C) and both a lower peak height and a faster decay in the CHO background (Fig. 2D). Dose-response experiments confirmed complete attenuation of CCL5-elicited arrestin 2 recruitment in both cellular backgrounds (Fig. 2, E and F), and reduced arrestin 3 recruitment (Fig. 2, G and H), particularly in the HEK-Arr2/3-KO background (Fig. 2H).

These results are broadly consistent with previous observations showing that arrestin recruitment is strongly attenuated in PD-CCR5 (Hüttenrauch et al., 2002), but indicate that isoform-related differences exist: whereas arrestin 2 recruitment is completely abrogated, arrestin 3 recruitment remains detectable in the HEK-Arr2/3-KO background and robust in the CHO background.

Arrestin Interaction Mutants Underline Importance of CCR5 Phosphorylation for Agonist-Driven Recruitment. According to the current model (Eichel et al., 2018; Kahsai et al., 2018; Latorraca et al., 2018), arrestins use two mechanisms to interact with activated GPCRs. The "tail interaction" involves destabilization of an internal ionic lock in the arrestin protein by the negatively charged phosphorylated C-terminal tail region of the receptor, leading to a conformational change in the arrestin protein that enables it to stably interact with the receptor C-terminal tail region (Eichel et al., 2018; Kahsai et al., 2018; Latorraca et al., 2018), and the "core interaction" involves docking of a conformationally flexible structure on the arrestin protein with structural motifs conserved across the GPCR superfamily that are revealed upon receptor activation (Eichel et al., 2018; Kahsai et al., 2018; Latorraca et al., 2018).

To investigate the relative contributions of the tail interaction and the core interaction on agonist-dependent recruitment of arrestins to CCR5, we next tested CCL5-induced recruitment to CCR5 of two previously characterized arrestin mutants in which the function of either interaction region has been disrupted (Fig. 3). R169E-Arr2, which carries a charge switch point mutation in the ionic lock module making it less dependent on receptor C-terminal tail phosphorylation for receptor engagement than its WT counterpart (Kovoor et al., 1999), exhibited increased CCL5-driven recruitment to PD-CCR5 compared with that of WT arrestin 2 (Fig. 3A), without affecting background levels of BRET signal obtained in the vehicle-only control (Fig. 3B). D70P–arrestin 3, which has been previously described as having an impaired core interaction (Chen et al., 2017), reduced CCL5-driven recruitment to WT CCR5 (Fig. 3C), with a further, almost complete reduction in signal on PD-CCR5 (Fig. 3D). These results provide further evidence of the importance of the tail interaction for CCL5-elicited recruitment of arrestin to CCR5, with the core interaction making a lower but nonetheless detectable contribution.

Role of Specific C-Terminal Serine Residues on Arrestin Recruitment to CCR5. Given the importance of the tail interaction to agonist-driven recruitment of arrestin to CCR5, and in the light of evidence that arrestin recruitment to certain GPCRs is driven by specific patterns of receptor phosphorylation (Yang et al., 2017; Sente et al., 2018), we next set out to investigate the impact on arrestin recruitment of substituting individual serine residues implicated in
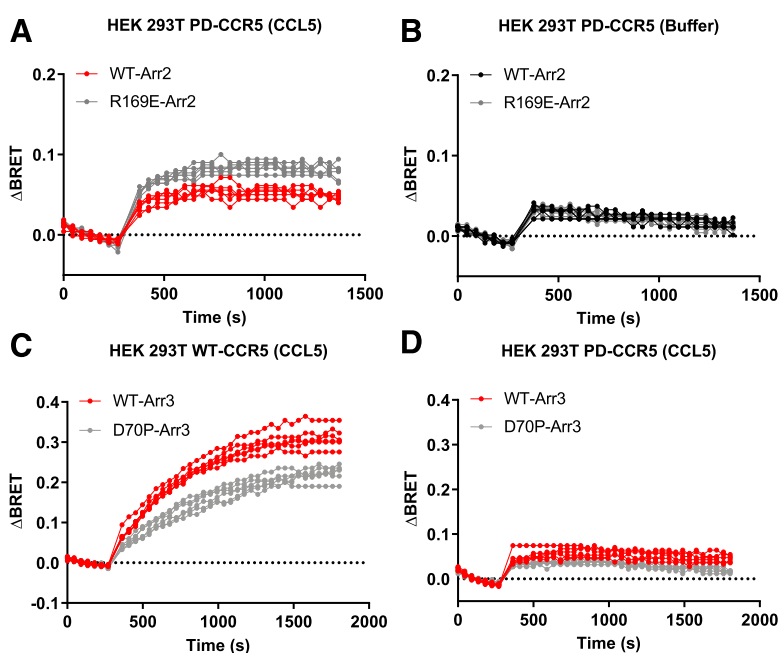
Fig. 3. CCL5-induced recruitment of arrestin interaction mutants to CCR5 and PD-CCR5. (A and B) BRET assays were performed by treating HEK-293T cells expressing PD-CCR5-RLuc8 together with YFP-Arr2 or YFP-R169E-Arr2 (as indicated) (A) with CCL5 at a concentration of 300 nM or with buffer (B), for 30 cycles of 45 seconds (chemokine addition after seven cycles). Data are shown as ΔBRET (AU). Individual traces of the time courses are shown ($n = 6$). (C and D) BRET assays were performed by treating HEK-293T cells expressing WT-CCR5-RLuc8 (C) or PD-CCR5-RLuc8 (D) together with YFP-Arr3 or YFP-D70P-Arr3 (as indicated) with CCL5 at a concentration of 300 nM for 40 cycles of 45 seconds (chemokine addition after seven cycles). Data are shown as ΔBRET (AU). Individual traces of the time courses are shown ($n = 6$).

agonist-driven CCR5 phosphorylation with alanine. We performed BRET-based arrestin recruitment assays, treating HEK cells expressing reporter constructs corresponding to each of the 16 different CCR5 Ser-Ala permutations with 300 nM CCL5 (Fig. 4).

Consistent with the previous experiments with WT and PD-CCR5 in the HEK-Arr2/3-KO and CHO backgrounds (Figs. 1 and 2), recruitment of both arrestin isoforms was strongly attenuated in PD-CCR5 in the HEK background (Fig. 4). With the exception of the S336A variant (ASSS), substitution of one or more C-terminal serines led to a statistically significant reduction in the level of arrestin 2 recruitment compared with that observed with the WT receptor (SSSS). For three of the variants carrying a single serine available for phosphorylation, Ser[336] (SAAA), Ser[342] (AASA), and Ser[349] (AAAS), and one carrying two serines available for phosphorylation Ser[342]/Ser[349] (AASS) signals were reduced to the level of PD-CCR5 (AAAA) (Fig. 4A; Supplemental Table 2). Similarly with arrestin 3, with the exception of the S336A variant (ASSS) and the S349A variant (SSSA), substitution of one or more C-terminal serines led to a statistically significant reduction in the level of recruitment compared with that observed with the WT receptor (SSSS), and three variants carrying a single serine available for phosphorylation, Ser[336] (SAAA), Ser[342] (AASA), and Ser[349] (AAAS), plus three carrying two serines available for phosphorylation, Ser[342]/Ser[349] (AASS) Ser[337]/Ser[349] (SAAS), and Ser[337]/Ser[342] (SASA), signals were reduced to the level of PD-CCR5 (AAAA) (Fig. 4B; Supplemental Table 2).

Arrestin Recruitment and CCR5 Phosphorylation Profiles of Highly Potent CCL5 Analogs. 5P12-RANTES, PSC-RANTES, and 5P14-RANTES are CCL5 analogs with potent anti-HIV activity, each with a distinct inhibitory mechanism (Table 1). There is evidence to suggest that the different inhibitory mechanisms of PSC-RANTES and 5P14-RANTES are due to differences in the extent and duration of arrestin recruitment that they elicit compared with native CCL5 (Bönsch et al., 2015). However, in the study concerned, recruitment of only one arrestin isoform was measured, ligands were tested at a single concentration, and methods for detection of arrestin recruitment were at best semiquantitative. We therefore set out to compare the nature and extent of arrestin recruitment elicited by the group of CCL5 analogs with that elicited by native CCL5, using both arrestin isoforms, a range of ligand concentrations, and BRET-based assays for quantitative readouts (Fig. 5).

PSC-RANTES Is a Superagonist for Arrestin Recruitment, and 5P14-RANTES Selectively Elicits Recruitment of Arr3 over Arr2 to CCR5. For both arrestin isoforms, and in both cellular backgrounds, PSC-RANTES elicited enhanced arrestin recruitment (Fig. 5, A–D). Recruitment was both more potent [fitted EC_{50} values of 8.2 nM (95% CI: 6.7–10 nM) versus 45 nM (95% CI: 28–73 nM) and 17 nM (95% CI: 12–22 nM) versus 52 nM (95% CI: 29–97 nM) for arrestin 2 (Fig. 5A) and arrestin 3 (Fig. 5C), respectively, on the HEK-Arr2/3-KO background, and 2.0 nM (95% CI: 1.5–2.5 nM) versus 90 nM (95% CI: 57–141 nM) (Fig. 5B) and 8.0 nM (95% CI: 6–11 nM) versus 30 nM (95% CI: 18–50 nM) (Fig. 5D), respectively, on the CHO background] and more efficacious [fitted E_{max} values of 1400 arbitrary units (AU) (95% CI: 1350–1460 AU) versus 420 AU (95% CI: 380–480 AU) and 1100 AU (95% CI: 1030–1170 AU) versus 450 AU (95% CI: 390–530 AU) for arrestin 2 (Fig. 5A) and 3 (Fig. 5C), respectively, on the HEK-Arr2/3-KO background, and 990 AU (95% CI: 960–1020 AU) versus 410 AU (95% CI: 380–440 AU) (Fig. 5B) and 870 AU (95% CI: 820–910 AU) versus 440 AU (95% CI: 400–500 AU) (Fig. 5D), respectively, on the CHO background] compared with native CCL5, confirming its previously described activity as a superagonist for arrestin recruitment to CCR5 (Bönsch et al., 2015). For 5P14-RANTES, more potent recruitment of both arrestin isoforms than native CCL5 was observed on both cell backgrounds [fitted EC_{50} values of 12 nM (95% CI: 9–17 nM) versus 45 nM (95% CI: 28–73 nM) and 26 nM (95% CI: 19–33 nM) versus 52 nM (95% CI: 29–97 nM for arrestin 2 (Fig. 5A) and 3 (Fig. 5C), respectively, on the HEK-Arr2/3-KO background and 2.5 nM (95% CI: 1.7–3.8 nM) versus 90 nM (95% CI: 57–141 nM) (Fig. 5B) and 10 nM (95% CI: 5.4–20 nM) (Fig. 5B) versus 30 nM (95% CI: 18–50 nM) (Fig. 5D), respectively, on the CHO background]. E_{max} levels were comparable on the HEK-Arr2/3-KO background [fitted E_{max} values of 440 AU (95% CI: 410–470 AU) versus 420 AU (95% CI: 380–480 AU) and 540
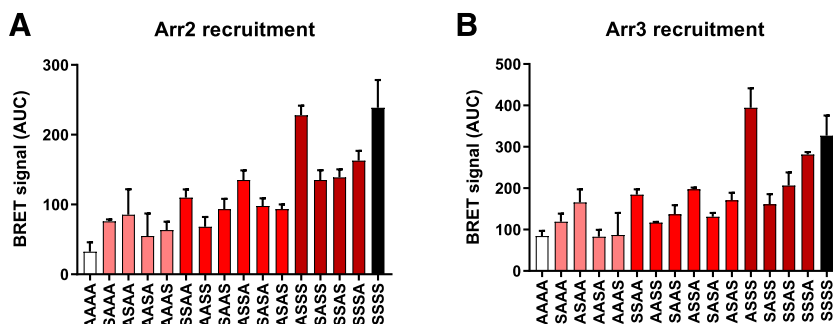
Fig. 4. CCL5-induced recruitment of arrestin 2 and arrestin 3 to 16 different CCR5 serine-to-alanine permutation mutants. HEK-293T cells were transfected with the indicated CCR5-RLuc8 serine-to-alanine permutation mutants together with either YFP-Arr2 or YFP-Arr3 (as indicated) and BRET signals obtained after treatment with CCL5 at a concentration of 300 nM were monitored over 30 minutes. Light through dark red colors indicate CCR5 variants carrying one, two, or three serines available for phosphorylation, with the codes indicating whether a serine or an alanine residue is present at each of the four positions (336, 337, 342, and 349). Data are shown as BRET signals (AUC, mean ± S.D.); $n = 3$ for all variants except for WT-CCR5 and PD-CCR5 ($n = 6$). For each variant, BRET signals were analyzed for statistical difference compared with both the WT-CCR5 and the PD-CCR5 signals using repeated measured one-way ANOVA with Dunnett's multiple comparisons tests (Supplemental Table 2). (A) Arrestin 2 recruitment: all signals statistically significantly different from the signal for WT-CCR5 (above) or PD-CCR5 (below) except those indicated. (B) Arrestin 3 recruitment: no signaling levels not statistically significantly different from that of WT-CCR5 (above) except where indicated; all signals statistically significantly different from the signal for PD-CCR5 (below) except those indicated.
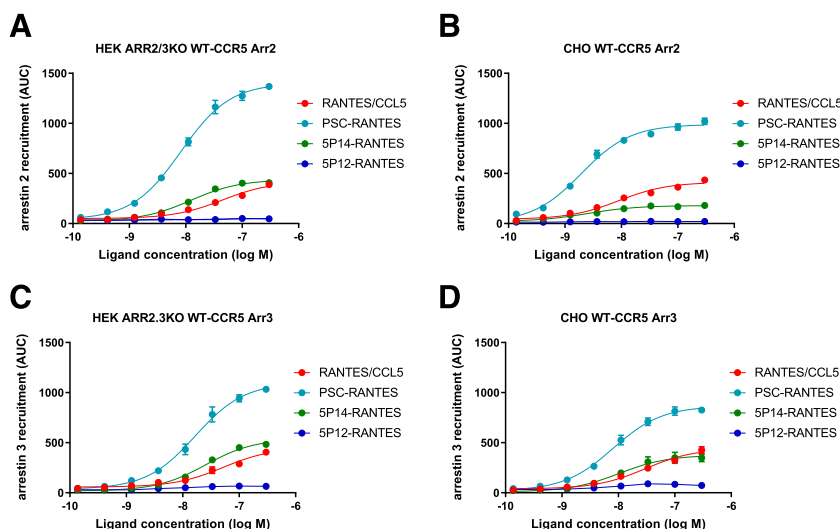
A

HEK ARR2/3KO WT-CCR5 Arr2

B

CHO WT-CCR5 Arr2

C

HEK ARR2.3KO WT-CCR5 Arr3

D

CHO WT-CCR5 Arr3

Fig. 5. Ligand-induced recruitment of arrestin 2 and arrestin 3 to WT-CCR5. BRET assays were performed by treating cells expressing WT-CCR5-RLuc8 together with YFP-Arr2 or YFP-Arr3 (as indicated) with chemokines and chemokine analogs at a concentration of 300 nM for 40 cycles of 45 seconds (chemokine addition after seven cycles). Data are shown as ΔBRET. ΔBRET is calculated by subtracting the average of the BRET signal (emission at 520 nm/emission at 475 nm) for the first seven cycles the BRET signal obtained for each time point. Individual traces of the time courses are shown ($n = 3$). BRET assays were performed by treating HEK-Arr2/3-KO or CHO cells expressing WT-CCR5-RLuc8 together with YFP-Arr2 or YFP-Arr3 (as indicated) with chemokines and chemokine analogs at the indicated concentrations for 40 cycles of 45 seconds (chemokine addition after seven cycles). Data are shown as AUC (mean ± S.D., $n = 3$). Fitted curves (for CCL5, PSC-RANTES, and 5P14-RANTES) were obtained by a non-linear regression analysis [log(agonist) vs. response (three parameters)] using Prism.

AU (95% CI: 510–580 AU) versus 450 AU (95% CI: 390–530 AU) for arrestin 2 (Fig. 5A) and 3 (Fig. 5C)]. Notably, however, we found evidence for isoform-selective arrestin recruitment by 5P14-RANTES in the CHO cell background, with an E_{max} level comparable to that of native CCL5 for arrestin 3 recruitment [fitted E_{max} values of 380 AU (95% CI: 330–430 AU) versus 440 AU (95% CI: 400–500 AU) (Fig. 5D)], but approximately 50% lower for arrestin 2 recruitment [fitted E_{max} values of 180 AU versus 410 AU (95% CI: 380–440 AU) (Fig. 5B)]. In agreement with its previous characterization as a ligand that does not elicit receptor internalization (Gaertner et al., 2008), 5P12-RANTES did not elicit recruitment of either arrestin isoform.

PSC-RANTES and 5P14-RANTES Differ in the Extent to which Core and Tail Interactions Are Implicated in Arrestin Recruitment. PSC-RANTES retains clearly detectable levels of recruitment of both arrestin isoforms on PD-CCR5 (Fig. 6, A–D), with the reduction in signal on PD-CCR5 compared with WT-CCR5 due to a lower plateau level of arrestin association in the HEK-Arr2/3-KO background (Fig. 6, E and G) and both a lower peak height and a faster decay in the CHO background (Fig. 6, F and H). As seen with native CCL5, PSC-RANTES-elicited recruitment of arrestin 2 to PD-CCR5 was increased for the phospho-insensitive R169E-Arr2 mutant (Fig. 7A), and levels of arrestin 3 recruitment to WT-CCR5 were diminished in the D70P-Arr3 core interaction mutant (Fig. 7C; Supplemental Table 3), indicating that both core and tail interactions play a role in CCR5-arrestin recruitment induced by PSC-RANTES. Notably, PSC-RANTES retains a level of arrestin recruitment when both core and tail domain interactions have been disrupted, with a clearly detectable level of arrestin recruitment for PSC-RANTES observed when the D70P-Arr3 core interaction mutant was combined with PD-CCR5 (Fig. 7D; Supplemental Table 3).

Establishment of the tail interaction appears to be crucial for 5P14-RANTES–elicited recruitment of both arrestin 2 and arrestin 3, since no recruitment of either isoform on either cell background is detectable on PD-CCR5 (Fig. 6). Recruitment of arrestin 2 to PD-CCR5 is partially rescued with the phospho-insensitive R169E-Arr2 mutant (Fig. 7B), and recruitment of

arrestin 3 to WT-CCR5 is reduced by the D70P-Arr3 core interaction mutant (Fig. 7E; Supplemental Table 3). These results indicate that the tail interaction is essential for 5P14-RANTES–elicited arrestin recruitment, with the core interaction, though incapable of driving arrestin recruitment by itself, being able to enhance recruitment elicited through the tail interaction.

CCL5 Analogs Do Not Differ from CCL5 in the Pattern of Receptor Phosphorylation That They Elicit. For certain GPCRs, the capacities of different ligands to modulate arrestin recruitment have been linked to differences in the pattern of receptor phosphorylation that they elicit (Nobles et al., 2011; Yang et al., 2017). We set out to investigate whether CCL5 analogs differ from native CCL5 in their capacity to elicit CCR5 phosphorylation at the four serine residues previously identified as targets for agonist-driven phosphorylation. First, we compared levels of receptor phosphorylation using a pair of anti-CCR5 phosphoserine antibodies, one whose binding is dependent on phosphorylation at Ser[349] and the other which requires phosphorylation at Ser[336]/Ser[337] for binding, in an ELISA assay performed on cell lysates after ligand treatment (100 nM, 1 hour). Our observations are consistent with previous reports (Oppermann et al., 1999; Pollok-Kopp et al., 2003), confirming that native CCL5 elicits phosphorylation at Ser[349] and Ser[336]/Ser[337] (Fig. 8, A and B), presumably in addition to Ser[342]. 5P14-RANTES elicits a phosphorylation profile comparable to that of CCL5, whereas PSC-RANTES, in line with previous reports (Bönsch et al., 2015), induces CCR5 hyperphosphorylation (Fig. 8, A and B; Supplemental Table 4). Neither PSC-RANTES nor 5P14-RANTES showed any apparent preference for phosphorylation at Ser[349] versus Ser[336]/Ser[337]. 5P12-RANTES did not elicit any detectable phosphorylation at either site.

We next compared the importance of individual CCR5 serine residues available for phosphorylation for arrestin recruitment elicited by PSC-RANTES (Fig. 8, C and D; Supplemental Table 5) and 5P14-RANTES (Fig. 8, E and F; Supplemental Table 6) using the panel of 16 CCR5 Ser-Ala mutants. Despite differences in overall arrestin recruitment levels, where PSC-RANTES elicited approximately 2-fold higher levels of recruitment than CCL5 and 5P14-RANTES,
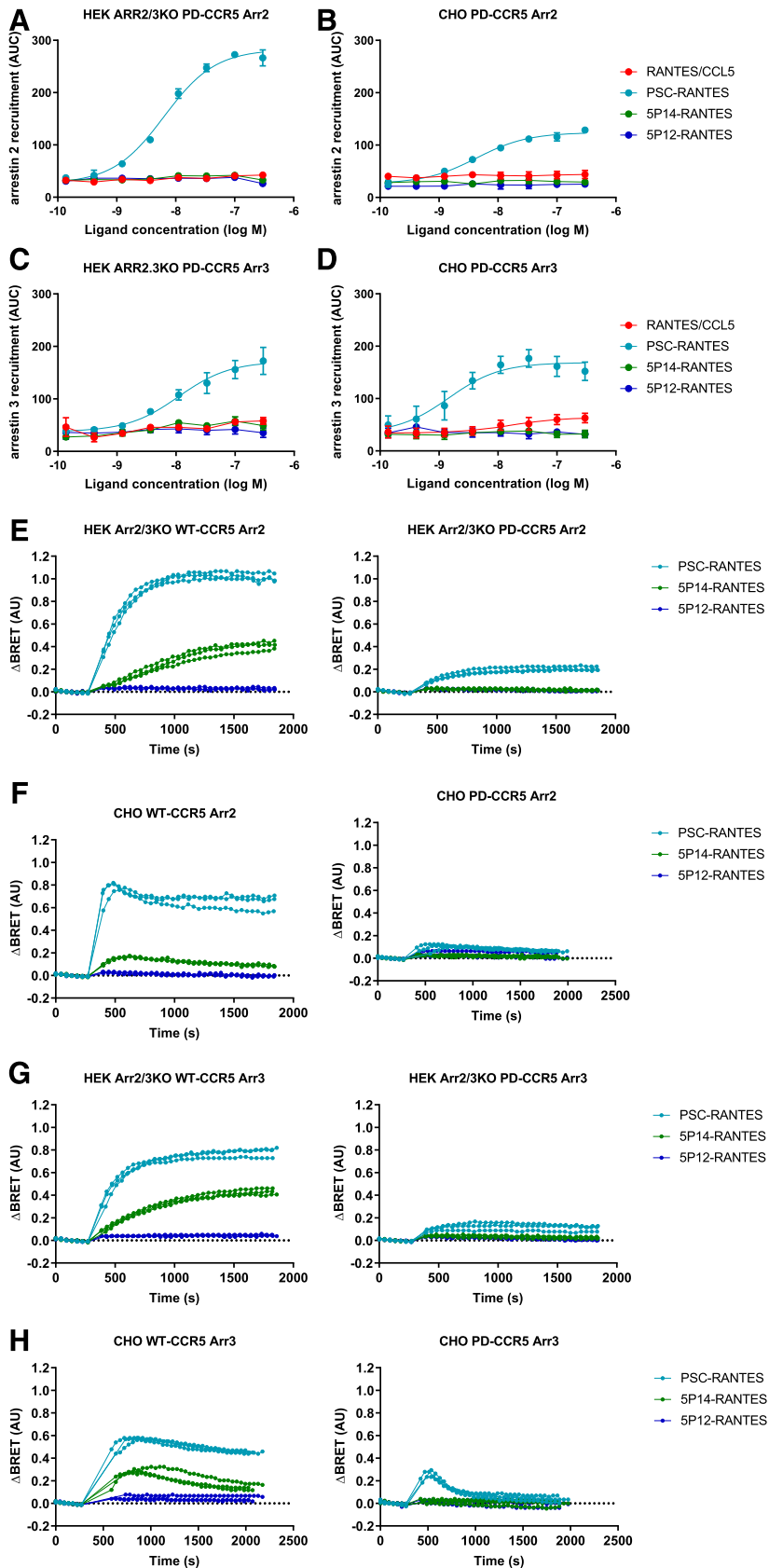
Fig. 6. Ligand-induced recruitment of arrestin 2 and arrestin 3 to PD-CCR5. BRET assays were performed by treating cells expressing PD-CCR5-RLuc8 together with YFP-Arr2 or YFP-Arr3 (as indicated) with chemokines and chemokine analogs at a concentration of 300 nM for 40 cycles of 45 seconds (chemokine addition after seven cycles). Data are shown as ΔBRET (AU). Individual traces of the time courses are shown ($n = 3$). (E–H) BRET assays were performed by treating HEK-Arr2/3-KO or CHO cells expressing PD-CCR5-RLuc8 together with YFP-Arr2 or YFP-Arr3 (as indicated) with chemokines and chemokine analogs at the indicated concentrations for 40 cycles of 45 seconds (chemokine addition after seven cycles). Data are shown as AUC (mean ± S.D., $n = 3$). Fitted curves [for CCL5 (H) and for PSC-RANTES (E–H)] were obtained by a nonlinear regression analysis [log(agonist) vs. response (three parameters)] using Prism.
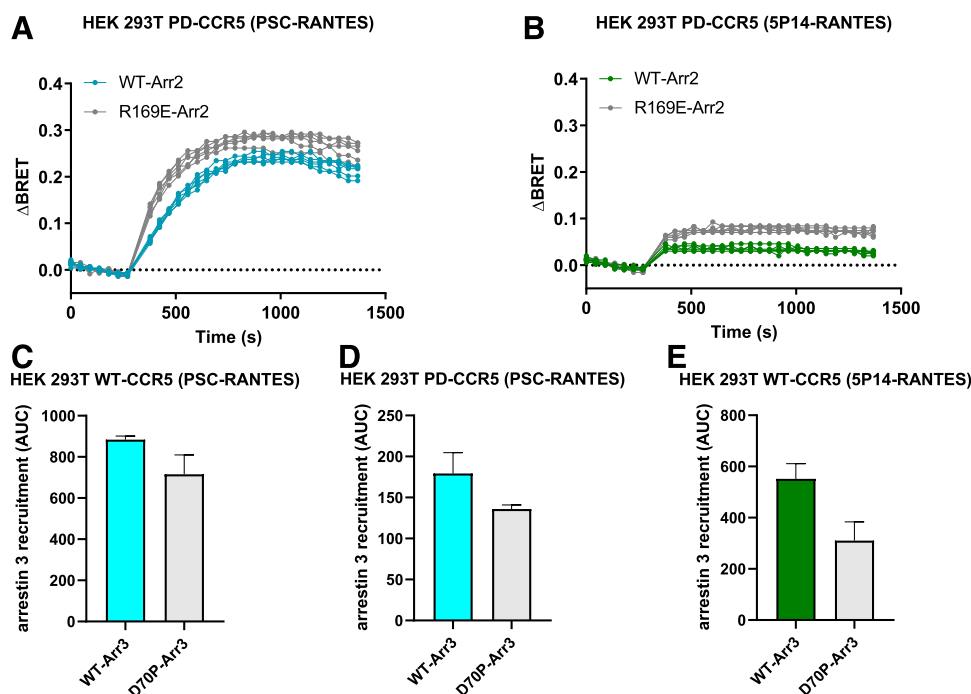
Fig. 7. Ligand-induced recruitment of arrestin interaction mutants to CCR5 and PD-CCR5. (A and B) BRET assays were performed by treating HEK-293T cells expressing PD-CCR5-RLuc8 together with YFP-Arr2 or YFP-R169E-Arr2 (as indicated) with PSC-RANTES (A) or 5P14-RANTES (B) at a concentration of 300 nM for 30 cycles of 45 seconds (chemokine addition after seven cycles). Data are shown as ΔBRET (AU). Individual traces of the time courses are shown ($n = 6$). (C and D) BRET assays were performed by treating HEK-293T cells expressing WT-CCR5-RLuc8 (C) or PD-CCR5-RLuc8 (D) together with YFP-Arr3 or YFP-D70P-Arr3 (as indicated) with PSC-RANTES at a concentration of 300 nM for 40 cycles of 45 seconds (chemokine addition after seven cycles). Data are shown as AUC (mean ± S.D., $n = 6$). (E) BRET assays were performed by treating HEK-293T cells expressing WT-CCR5-RLuc8 together with YFP-Arr3 or YFP-D70P-Arr3 (as indicated) with PSC-RANTES at a concentration of 300 nM for 40 cycles of 45 seconds (chemokine addition after seven cycles). Data are shown as AUC (mean ± S.D., $n = 6$). (C–E) BRET signals of WT-Arr3 recruitment were analyzed for statistical difference compared with those of D70P-Arr3 recruitment using unpaired t tests with Welch's correction (Supplemental Table 3).

relative levels of arrestin recruitment across the panel for the two CCL5 analogs were very similar to each other and to those of native CCL5 (Fig. 1). These results indicate that the capacity of PSC-RANTES to elicit CCR5 hyperphosphorylation contributes to its enhanced capacity to elicit arrestin recruitment, but neither PSC-RANTES nor 5P14-RANTES elicit ligand-selective receptor phosphorylation patterns.

Discussion

A Complete Survey of Native Ligand-Driven CCR5-Arrestin Recruitment and Its Dependence on Receptor Phosphorylation. Previous studies have implicated both receptor phosphorylation and recruitment of arrestin 2 and arrestin 3 in the process of CCR5 desensitization driven by its natural agonists (Hüttenrauch et al., 2005). In this work, however, measurement of arrestin recruitment was limited to semiquantitative approaches at a limited number of fixed timepoints (Hüttenrauch et al., 2005), and a single antibody was used to detect recruitment of both arrestin isoforms (Hüttenrauch et al., 2002, 2005). In this study we used separate sensitive BRET-based arrestin recruitment assays to measure levels of recruitment of each arrestin isoform in real time and in living cells, using WT-CCR5 as well as two previously described arrestin mutants (Kovoor et al., 1999; Chen et al., 2017) in order investigate the relative importance of tail and core interactions for association of CCR5 with arrestins. Our results demonstrate that CCL5 elicits similar levels of recruitment for both arrestin isoforms

(Fig. 1) and that although the core interaction makes a contribution, arrestin recruitment is strongly dependent on the tail interaction, particularly in the case of arrestin 2 (Fig. 2). The relative tolerance of arrestin 3 recruitment to unphosphorylated receptors compared with that of arrestin 2 has been noted for other GPCRs and is proposed to relate to structural differences between the two isoforms (Zhan et al., 2011). Some differences in ligand-induced arrestin-receptor association and dissociation kinetics in the CHO versus the HEK cell backgrounds were noted (Figs. 1 and 6). This variation might be due to differences in post-translational modification in the extracellular domains of CCR5, which are known to contribute to the binding affinity of CCR5 ligands (Bannert et al., 2001) and/or to differences in the levels and composition of cytosolic receptor and arrestin-binding proteins in the two cellular backgrounds.

The importance of receptor phosphorylation at distinct serine sites for arrestin recruitment has been investigated using CCR5 Ser-Ala mutants in a previous study, but this study did not cover all possible serine residue permutations. In this study we generated a complete set of 16 Ser-Ala variants covering all possible permutations across the four phosphorylated serine positions. In agreement with the previous work (Hüttenrauch et al., 2002), we noted that levels of arrestin recruitment generally correlate with the number of serine residues available for phosphorylation, irrespective of their position in the sequence (Fig. 4). Nonetheless, our results indicate that a certain level of sensitivity to the localization of serine phosphorylation does exist, however. CCR5 variants
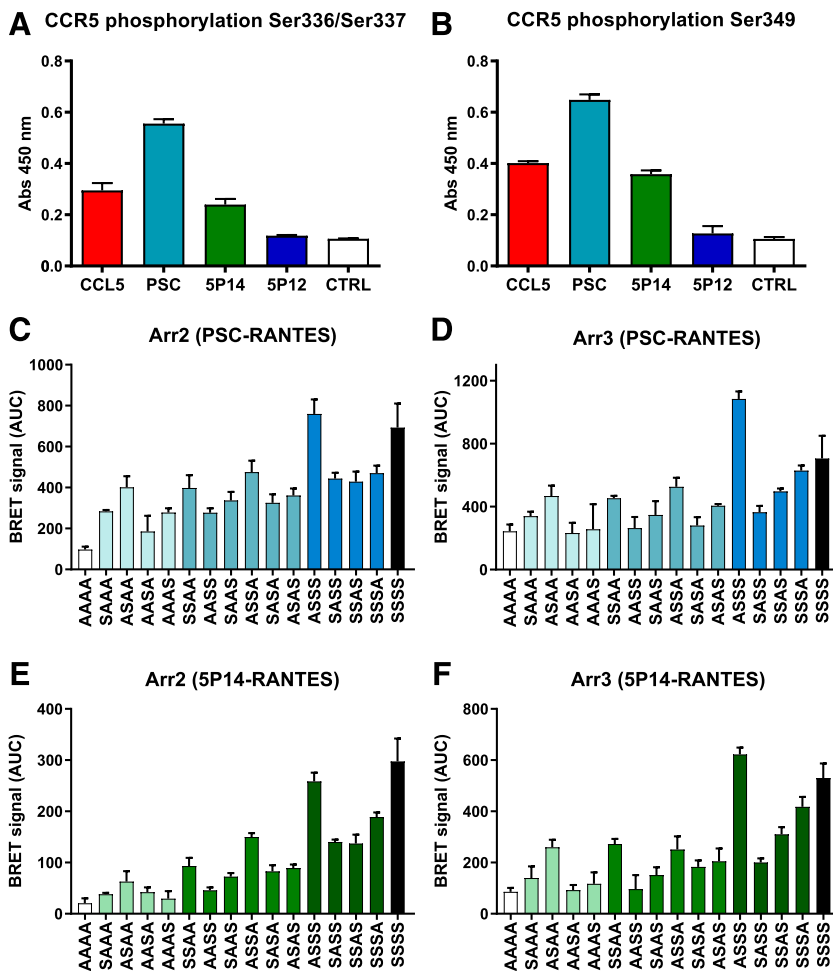
Fig. 8. (A and B) Ligand-induced CCR5 C-terminal phosphorylation. CHO cells stably expressing CCR5 (CHO-CCR5) were treated with 100 nM of chemokines and chemokine analogs for 1 hour at 37°C. CCR5 C-terminal phosphorylation was quantified using recombinant phospho-specific monoclonal anti-CCR5 antibodies (0.5 μg/ml). Data are shown as mean absorbance at 450 nm (Abs 450 nm, mean ± S.D.); $n = 3$. Absorbance signals were analyzed for statistically significant difference from both the RANTES/CCL5 and no treatment signals using repeated measured one-way ANOVA with Dunnett's multiple comparisons tests (Supplemental Table 4). (C–F) Ligand-induced recruitment of arrestin 2 and arrestin 3–16 CCR5 serine-to-alanine permutation mutants. HEK-293T were transfected with the indicated CCR5-RLuc8 serine-to-alanine permutation mutants together with either YFP-Arr2 or YFP-Arr3 (as indicated), and BRET signals obtained after treatment with the indicated chemokine analogs at a concentration of 300 nM were monitored over 30 minutes. Light through dark blue/green colors indicate CCR5 variants carrying one, two, or three serine residues available for phosphorylation, with the codes indicating whether a serine or an alanine residue is present at each of the four positions (336, 337, 342, and 349). Data are shown as BRET signals (AUC, mean ± S.D.); $n = 3$ for all variants except for WT-CCR5 and PD-CCR5 ($n = 6$). For each variant, BRET signals were analyzed for statistical difference compared with both the WT-CCR5 and the PD-CCR5 signals using repeated measured one-way ANOVA with Dunnett's multiple comparisons tests (Supplemental Tables 5 and 6).

lacking one of the four serine residues available for phosphorylation differ in their capacity for arrestin recruitment, with Ser[337] and Ser[342] apparently more important for full recruitment capacity than Ser[336] and Ser [349]. Furthermore, in CCR5 variants possessing one or two serine residues available for phosphorylation, those in which Ser[337] is present tended more toward increased capacity for arrestin recruitment than variants in which it was absent (Fig. 4).

Further Elucidation of the Inhibitory Mechanisms of CCL5 Analogs with Potent Anti-HIV Activity. Having characterized arrestin recruitment to CCR5 elicited by native CCL5, we were able to determine the extent to which potent anti-HIV CCL5 analogs differ from the parent chemokine in terms of the quantity and quality of arrestin recruitment they elicit. In line with previous observations (Bönsch et al., 2015), our results indicate that arrestin recruitment does not play a role in the inhibitory mechanism of 5P12-RANTES (Fig. 5), a ligand that neither activates CCR5 nor induces its endocytosis (Gaertner et al., 2008). This parameter is an important component of the safety profile of 5P12-RANTES, which has been taken into clinical development as an HIV prevention medicine (Hartley et al., 2004; Cerini et al., 2017), since arrestin signaling could lead to cellular responses with physiologic effects that are currently unknown.

We observed that PSC-RANTES, previously described as a CCR5 superagonist, elicits increased recruitment of both arrestin isoforms compared with the parent chemokine

(Fig. 5). This phenomenon, in agreement with previous observations (Hartley et al., 2004), would explain the enhanced capacity of PSC-RANTES to elicit CCR5 sequestration. As with CCL5, arrestin recruitment mediated by PSC-RANTES is strongly dependent on the tail interaction (Fig. 6). We noted, however, that PSC-RANTES retains a considerable level of arrestin recruitment activity on PD-CCR5 (Fig. 6), suggesting that it is capable of inducing CCR5 conformations that promote the arrestin core interaction more powerfully than those elicited by native CCL5. Our observation that the Arr3-D70P core mutant only partially abrogated PSC-RANTES-elicited arrestin recruitment to PD-CCR5 (Fig. 7) might simply be because the mutation does not completely abrogate the core interaction. Alternatively, PSC-RANTES could potentially be capable of eliciting phosphorylation at additional sites to the four serine residues that were previously shown to be phosphorylated in response to native ligands (Oppermann et al., 1999) and that were alanine-substituted in PD-CCR5. In this regard, the cytoplasmic domain of CCR5 contains several potentially available serine and threonine residues: Ser[63] and Thr[65] in the first intracellular loop, as well as Ser[325], Thr[340], and Thr[343] in the C-terminal tail. PSC-RANTES drives CCR5 hyperphosphorylation (Fig. 8, A and B) with the resulting arrestin recruitment, as with the parent chemokine, not showing any absolute requirement for particular serine residues in the receptor C-terminal domain (Fig. 8, C

and E). Presumably, PSC-RANTES elicits CCR5 conformations that recruit and activate GPCR kinases more effectively than those adopted by the receptor in response to the parent chemokine.

We observed that although 5P14-RANTES elicits comparable E_{max} levels of arrestin 3 recruitment to the parent chemokine, its EC_{50} values are clearly lower (Fig. 5, C and D). Hence, although 5P14-RANTES shows similar functional efficacy to that of CCL5 for arrestin 3 recruitment to CCR5, its functional potency is higher. A possible interpretation of this observation is that when bound, 5P14-RANTES elicits CCR5 conformations with similar arrestin recruitment efficacies to those adopted by CCR5 bound to native CCL5, but that 5P14-RANTES has higher CCR5 binding affinity and can engage CCR5 at lower concentrations.

Similarly, we noted comparable E_{max} levels but lower EC_{50} values with respect to the parent chemokine for 5P14-RANTES–mediated arrestin 2 recruitment on the HEK-Arr2/3-KO background (Fig. 5A). Strikingly, however, we observed in CHO background that although 5P14-RANTES is more potent for inducing arrestin 2 recruitment the parent chemokine, its efficacy is approximately 50% lower (Fig. 5B). A possible interpretation of this observation is that in the CHO background, the conformations adopted by CCR5 engaged by 5P14-RANTES have a lower arrestin 2 recruitment capacity than those adopted by CCR5 engaged by the parent chemokine.

These observations are consistent with those of Bönsch et al. (2015), who noted using pull-down assays and fluorescence microscopy that 5P14-RANTES elicits lower levels of CCR5-Arr2 association than native CCL5. Arrestin isoform-selective recruitment by a ligand is uncommon in GPCRs studied to date (Hoffmann et al., 2008; Groer et al., 2011; Pradhan et al., 2016). It could potentially be a mechanism underlying the ligand-selective postendocytic sorting phenomenon that was previously observed for 5P14-RANTES in the same cellular background (Bönsch et al., 2015).

Arrestin recruitment elicited by 5P14-RANTES is fully dependent on the arrestin tail interaction. Although arrestin 3 recruitment for both 5P14-RANTES and CCL5 is abrogated on PD-CCR5, 5P14-RANTES differs from the parent chemokine in that it is unable to elicit recruitment of arrestin 3 to PD-CCR5 either (Fig. 6). This complete dependence on arrestin tail interaction provides another potential explanation for the previously observed differences in postendocytic sorting of CCR5 driven by the two ligands (Bönsch et al., 2015), since arrestins can adopt different conformations according to the extent of core versus tail interaction (Nobles et al., 2011; Chen et al., 2017), and these different conformations can in turn modulate the activity of arrestin as an adaptor protein, changing the repertoire of downstream effector proteins that are recruited and hence possibly affecting receptor trafficking pathways (Srivastava et al., 2015).

For certain GPCRs, differences in ligand-elicited arrestin interaction have been linked to differences in the extent and localization of ligand-elicited phosphorylation of the receptor C-terminal domain (Kohout et al., 2004), but this does not appear to be the case for 5P14-RANTES and CCR5, since both the overall level of phosphorylation it elicits (Fig. 8, A and B) and its dependence on the availability of serine residues at different CCR5 C-terminal domain positions (Fig. 8, D and F) are very similar to those of the parent chemokine.

In this study we have provided the first complete survey of native ligand-elicited CCR5 arrestin recruitment, taking account of the current two-module model for arrestin-GPCR interaction, and obtained comparative data for three potent anti-HIV chemokine analogs, one of which is currently in clinical development. It is important to note that the BRET-based data obtained in this study made use of systems in which the overexpressed receptor and arrestin constructs were present at levels that differed across the different cell systems used (Supplemental Figs. 1 and 2; Supplemental Table 6) and are likely to be higher than typical endogenous levels in physiologic cells. Nonetheless, these observations will help to further elucidate the pharmacology and cell biology of CCR5 and support work to develop new inhibitors both of this important drug target and of the family of chemokine receptors to which it belongs.

Authorship Contributions

Participated in research design: Martins, Hartley.

Conducted experiments: Martins, Brodier, Rossitto-Borlat.

Contributed new reagents or analytic tools: Martins, Brodier, Ilgaz, Villard.

Performed data analysis: Martins, Hartley.

Wrote or contributed to the writing of the manuscript: Martins, Hartley.

References

Aldinucci D and Casagrande N (2018) Inhibition of the CCL5/CCR5 axis against the progression of gastric cancer. *Int J Mol Sci* **19**:1477.

Alvarez CE (2008) On the origins of arrestin and rhodopsin. *BMC Evol Biol* **8**:222.

Alvarez-Curto E, Inoue A, Jenkins L, Raihan SZ, Prihandoko R, Tobin AB, and Milligan G (2016) Targeted elimination of G proteins and arrestins defines their specific contributions to both intensity and duration of G protein-coupled receptor signaling. *J Biol Chem* **291**:27147–27159.

Bannert N, Craig S, Farzan M, Sogah D, Santo NV, Choe H, and Sodroski J (2001) Sialylated O-glycans and sulfated tyrosines in the NH2-terminal domain of CC chemokine receptor 5 contribute to high affinity binding of chemokines. *J Exp Med* **194**:1661–1673.

Bönsch C, Munteanu M, Rossitto-Borlat I, Fürstenberg A, and Hartley O (2015) Potent anti-HIV chemokine analogs direct post-endocytic sorting of CCR5. *PLoS One* **10**:e0125396.

Carrington M, Dean M, Martin MP, and O'Brien SJ (1999) Genetics of HIV-1 infection: chemokine receptor CCR5 polymorphism and its consequences. *Hum Mol Genet* **8**:1939–1945.

Cerini F, Offord R, McGowan I, and Hartley O (2017) Stability of 5P12-RANTES, a candidate rectal microbicide, in human rectal lavage. *AIDS Res Hum Retroviruses* **33**:768–777.

Chen C-H, Paing MM, and Trejo J (2004) Termination of protease-activated receptor-1 signaling by β-arrestins is independent of receptor phosphorylation. *J Biol Chem* **279**:10020–10031.

Chen Q, Perry NA, Vishnivetskiy SA, Berndt S, Gilbert NC, Zhuo Y, Singh PK, Tholen J, Ohi MD, Gurevich EV, et al. (2017) Structural basis of arrestin-3 activation and signaling. *Nat Commun* **8**:1427.

Colin P, Bénureau Y, Staropoli I, Wang Y, Gonzalez N, Alcami J, Hartley O, Brelot A, Arenzana-Seisdedos F, and Lagane B (2013) HIV-1 exploits CCR5 conformational heterogeneity to escape inhibition by chemokines. *Proc Natl Acad Sci USA* **110**: 9475–9480.

DeWire SM, Ahn S, Lefkowitz RJ, and Shenoy SK (2007) Beta-arrestins and cell signaling. *Annu Rev Physiol* **69**:483–510.

Eichel K, Jullié D, Barsi-Rhyne B, Latorraca NR, Masureel M, Sibarita J-B, Dror RO, and von Zastrow M (2018) Catalytic activation of β-arrestin by GPCRs. *Nature* **557**: 381–386.

Eichel K and von Zastrow M (2018) Subcellular organization of GPCR signaling. *Trends Pharmacol Sci* **39**:200–208.

Escola JM, Kuenzi G, Gaertner H, Foti M, and Hartley O (2010) CC chemokine receptor 5 (CCR5) desensitization: cycling receptors accumulate in the trans-Golgi network. *J Biol Chem* **285**:41772–41780.

Gaertner H, Cerini F, Escola JM, Kuenzi G, Melotti A, Offord R, Rossitto-Borlat I, Nedellec R, Salkowitz J, Gorochov G, et al. (2008) Highly potent, fully recombinant anti-HIV chemokines: reengineering a low-cost microbicide. *Proc Natl Acad Sci USA* **105**:17706–17711.

Gallo SA, Finnegan CM, Viard M, Raviv Y, Dimitrov A, Rawat SS, Puri A, Durell S, and Blumenthal R (2003) The HIV Env-mediated fusion reaction. *Biochim Biophys Acta* **1614**:36–50.

Gimenez LE, Kook S, Vishnivetskiy SA, Ahmed MR, Gurevich EV, and Gurevich VV (2012) Role of receptor-attached phosphates in binding of visual and non-visual arrestins to G protein-coupled receptors. *J Biol Chem* **287**:9028–9040.

Groer CE, Schmid CL, Jaeger AM, and Bohn LM (2011) Agonist-directed interactions with specific beta-arrestins determine mu-opioid receptor trafficking, ubiquitination, and dephosphorylation. *J Biol Chem* **286**:31731–31741.

Gurevich VV and Gurevich EV (2006) The structural basis of arrestin-mediated regulation of G-protein-coupled receptors. *Pharmacol Ther* **110**:465–502.

Hartley O, Gaertner H, Wilken J, Thompson D, Fish R, Ramos A, Pastore C, Dufour B, Cerini F, Melotti A, et al. (2004) Medicinal chemistry applied to a synthetic protein: development of highly potent HIV entry inhibitors. *Proc Natl Acad Sci USA* **101**:16460–16465.

Hoffmann C, Ziegler N, Reiner S, Krasel C, and Lohse MJ (2008) Agonist-selective, receptor-specific interaction of human P2Y receptors with beta-arrestin-1 and -2. *J Biol Chem* **283**:30933–30941.

Hüttenrauch F, Nitzki A, Lin F-T, Höning S, and Oppermann M (2002) β-arrestin binding to CC chemokine receptor 5 requires multiple C-terminal receptor phosphorylation sites and involves a conserved Asp-Arg-Tyr sequence motif. *J Biol Chem* **277**:30769–30777.

Hüttenrauch F, Pollok-Kopp B, and Oppermann M (2005) G protein-coupled receptor kinases promote phosphorylation and beta-arrestin-mediated internalization of CCR5 homo- and hetero-oligomers. *J Biol Chem* **280**:37503–37515.

Jala VR, Shao W-H, and Haribabu B (2005) Phosphorylation-independent β-arrestin translocation and internalization of leukotriene B4 receptors. *J Biol Chem* **280**:4880–4887.

Jin J, Colin P, Staropoli I, Lima-Fernandes E, Ferret C, Demir A, Rogée S, Hartley O, Randriamampita C, Scott MG, et al. (2014) Targeting spare CC chemokine receptor 5 (CCR5) as a principle to inhibit HIV-1 entry. *J Biol Chem* **289**:19042–19052.

Kahsai AW, Pani B, and Lefkowitz RJ (2018) GPCR signaling: conformational activation of arrestins. *Cell Res* **28**:783–784.

Kohout TA, Nicholas SL, Perry SJ, Reinhart G, Junger S, and Struthers RS (2004) Differential desensitization, receptor phosphorylation, beta-arrestin recruitment, and ERK1/2 activation by the two endogenous ligands for the CC chemokine receptor 7. *J Biol Chem* **279**:23214–23222.

Kovoor A, Celver J, Abdryashitov RI, Chavkin C, and Gurevich VV (1999) Targeted construction of phosphorylation-independent β-arrestin mutants with constitutive activity in cells. *J Biol Chem* **274**:6831–6834.

Kraft K, Olbrich H, Majoul I, Mack M, Proudfoot A, and Oppermann M (2001) Characterization of sequence determinants within the carboxyl-terminal domain of chemokine receptor CCR5 that regulate signaling and receptor internalization. *J Biol Chem* **276**:34408–34418.

Latorraca NR, Wang JK, Bauer B, Townshend RJL, Hollingsworth SA, Olivieri JE, Xu HE, Sommer ME, and Dror RO (2018) Molecular mechanism of GPCR-mediated arrestin activation. *Nature* **557**:452–456.

Lefkowitz R (2007) Introduction to special section on β-arrestins. *Annu Rev Physiol* **69**:451.

Loening AM, Fenn TD, Wu AM, and Gambhir SS (2006) Consensus guided mutagenesis of Renilla luciferase yields enhanced stability and light output. *Protein Eng Des Sel* **19**:391–400.

Lois C, Hong EJ, Pease S, Brown EJ, and Baltimore D (2002) Germline transmission and tissue-specific expression of transgenes delivered by lentiviral vectors. *Science* **295**:868–872.

Martin-Blondel G, Brassat D, Bauer J, Lassmann H, and Liblau RS (2016) CCR5 blockade for neuroinflammatory diseases--beyond control of HIV. *Nat Rev Neurol* **12**:95–105.

Naldini L, Blömer U, Gallay P, Ory D, Mulligan R, Gage FH, Verma IM, and Trono D (1996) In vivo gene delivery and stable transduction of nondividing cells by a lentiviral vector. *Science* **272**:263–267.

Nobles KN, Xiao K, Ahn S, Shukla AK, Lam CM, Rajagopal S, Strachan RT, Huang TY, Bressler EA, Hara MR, et al. (2011) Distinct phosphorylation sites on the β(2)-adrenergic receptor establish a barcode that encodes differential functions of β-arrestin. *Sci Signal* **4**:ra51.

Oppermann M, Mack M, Proudfoot AE, and Olbrich H (1999) Differential effects of CC chemokines on CC chemokine receptor 5 (CCR5) phosphorylation and identification of phosphorylation sites on the CCR5 carboxyl terminus. *J Biol Chem* **274**: 8875–8885.

Peterson YK and Luttrell LM (2017) The diverse roles of arrestin scaffolds in G protein-coupled receptor signaling. *Pharmacol Rev* **69**:256–297.

Pollok-Kopp B, Schwarze K, Baradari VK, and Oppermann M (2003) Analysis of ligand-stimulated CC chemokine receptor 5 (CCR5) phosphorylation in intact cells using phosphosite-specific antibodies. *J Biol Chem* **278**:2190–2198.

Pradhan AA, Perroy J, Walwyn WM, Smith ML, Vicente-Sanchez A, Segura L, Bana A, Kieffer BL, and Evans CJ (2016) Agonist-specific recruitment of arrestin isoforms differentially modify delta opioid receptor function. *J Neurosci* **36**:3541–3551.

Rajagopal S and Shenoy SK (2018) GPCR desensitization: acute and prolonged phases. *Cell Signal* **41**:9–16.

Richardson MD, Balius AM, Yamaguchi K, Freilich ER, Barak LS, and Kwatra MM (2003) Human substance P receptor lacking the C-terminal domain remains competent to desensitize and internalize. *J Neurochem* **84**:854–863.

Sente A, Peer R, Srivastava A, Baidya M, Lesk AM, Balaji S, Shukla AK, Babu MM, and Flock T (2018) Molecular mechanism of modulating arrestin conformation by GPCR phosphorylation. *Nat Struct Mol Biol* **25**:538–545.

Srivastava A, Gupta B, Gupta C, and Shukla AK (2015) Emerging functional divergence of β-arrestin isoforms in GPCR function. *Trends Endocrinol Metab* **26**: 628–642.

Trkola A, Paxton WA, Monard SP, Hoxie JA, Siani MA, Thompson DA, Wu L, Mackay CR, Horuk R, and Moore JP (1998) Genetic subtype-independent inhibition of human immunodeficiency virus type 1 replication by CC and CXC chemokines. *J Virol* **72**:396–404.

Wong MM and Fish EN (2003) Chemokines: attractive mediators of the immune response. *Semin Immunol* **15**:5–14.

Yang Z, Yang F, Zhang D, Liu Z, Lin A, Liu C, Xiao P, Yu X, and Sun J-P (2017) Phosphorylation of G protein-coupled receptors: from the barcode hypothesis to the flute model. *Mol Pharmacol* **92**:201–210.

Zhan X, Gimenez LE, Gurevich VV, and Spiller BW (2011) Crystal structure of arrestin-3 reveals the basis of the difference in receptor binding between two non-visual subtypes. *J Mol Biol* **406**:467–478.

Zheng Y, Han GW, Abagyan R, Wu B, Stevens RC, Cherezov V, Kufareva I, and Handel TM (2017) Structure of CC chemokine receptor 5 with a potent chemokine antagonist reveals mechanisms of chemokine recognition and molecular mimicry by HIV. *Immunity* **46**:1005–1017.e5.

Address correspondence to: Oliver Hartley, Department of Pathology and Immunology, Faculty of Medicine, University of Geneva, 1 Rue Michel-Servet, 1205 Geneva, Switzerland. E-mail: oliver.hartley@unige.ch